

Ka-band Triangular Patch Antenna on Micromachined High-K Substrate

Preeti Sharma¹, #Shiban K. Koul¹ and Sudhir Chandra¹

¹Centre for Applied Research in Electronics (CARE), Indian Institute of Technology, Hauz Khas, New Delhi –110016, INDIA
preeti5_sharma@yahoo.com, # shiban_koul@hotmail.com, schandra@care.iitd.ernet.in

Abstract

This paper reports the design of a Ka-band Equilateral triangular patch antenna (ETPA) fabricated using post-CMOS and post-MMIC compatible process technology. The antenna uses an air-cavity underneath the patch radiator that is supported on thin dielectric membrane. The antenna structure was analysed and optimised using the finite element method (FEM) based Agilent High Frequency Structure Simulator (version 5.5). The fabricated antenna resonated at 34.3 GHz with -10 return loss bandwidth of 1.2 GHz.

1. INTRODUCTION

Triangular patch antennas are found to provide radiation characteristics similar to those of rectangular patch antennas, but with a smaller physical size. Many researchers have published work on determining the resonant frequency of the equilateral triangular patch antenna excited in the dominant mode [1,2]. In almost every paper reported, the patches are excited with coaxial-probe at some distance d from the tip of the triangle. To realize this antenna at high frequencies, it is better to design the feed network using planar transmission line. Moreover it would be advantageous if this antenna were fabricated using microwave monolithic integrated circuits (MMICs) compatible substrates such as single-crystal silicon ($\epsilon_r=11.9$).

Patch antennae are generally fabricated on somewhat low dielectric constant ($\epsilon_r \leq 10$) and thick substrates to ensure good radiation efficiency and larger impedance bandwidth of the antenna. With the development of monolithic microwave integrated circuit (MMIC) technology, it would be advantageous if antennas can be fabricated on high dielectric constant ($\epsilon_r \geq 10$) substrates such as silicon and gallium arsenide. Microstrip antennae fabricated on high dielectric constant substrates can be easily integrated with MMIC RF front-end circuitry. There are essentially two major factors that limits the performance of an antenna fabricated on high-index ($\epsilon_r = 11.9$) silicon substrates. They are (i) excitation of surface waves that result in narrow bandwidth, poor radiation efficiency and degraded radiation patterns, and (ii) losses caused by silicon conductivity. Using silicon-micromachining technology, we can solve the first problem [3]. Here, the bulk silicon material is removed underneath the patch radiator as shown in Fig.1 (a) to synthesize a locally low dielectric constant ($\epsilon_r = 1$) region around the antenna. The second

problem is overcome by using a High Resistivity Silicon (HRS) substrate, where the losses due to the substrate conductivity are minimized, thereby, improving the antenna radiation efficiency.

In present case, we have fed the antenna at the center of one of the side-length of an equilateral triangle as shown in Fig.1 (b). And to make it MMIC compatible with low-loss characteristics, we have realized triangular patch antenna suspended on thin dielectric membrane using RF sputtering and bulk silicon micromachining.

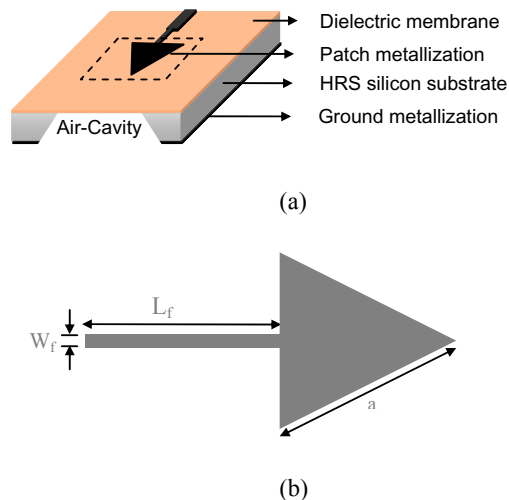


Fig. 1: (a) Schematic of micromachined triangular patch antenna suspended on thin dielectric membrane (b) Conductor pattern

2. ANTENNA MODELING

Consider the micromachined triangular patch antenna suspended on thin dielectric membrane with microstrip feed shown in Fig.1. Initially, the effective side length “ a_e ” of the equilateral triangular patch antenna for the TM_{10} mode was calculated using the empirical formula given by (1)[4].

$$a_e = \frac{2c}{3f_r \sqrt{\epsilon_{\text{reff}}}} \quad (1)$$

where,

3. FABRICATION OF THE ANTENNA

$$a_e = a \left[\begin{array}{l} 1 + 2.199 \frac{h}{a} - 12853 \frac{h}{a \sqrt{\epsilon_{\text{reff}}}} + 16436 \frac{h}{a \epsilon_{\text{reff}}} + 6.182 \left(\frac{h}{a} \right)^2 \\ - 9.802 \frac{1}{\sqrt{\epsilon_{\text{reff}}}} \left(\frac{h}{a} \right)^2 \end{array} \right]^2 \quad (2)$$

Here, f_r is the resonant frequency of the antenna, c is the velocity of light in free space. ϵ_{reff} is the effective permittivity of the multi-layer structure consisting of the dielectric membrane on air-cavity. The value of ϵ_{reff} is taken as unity for the initial calculations. a and h are the side-length of the triangle and substrate thickness, respectively. In the present case, when fed at the centre of one of the edges of the triangle, the input impedance is close to 50Ω . Therefore no additional transformer section is used for matching the antenna to the feed line.

The antenna structure was next analyzed and optimized using the finite-element method (FEM) based software Agilent High Frequency Structure Simulator (version 5.5) [5]. The multi-layer antenna structure used in the simulation is shown in Fig. 2(a). The optimized return loss characteristics of the antenna structure shown in Fig. 2(a) are plotted in Fig. 2(b). Table-1 gives the dimensions of optimized antenna designed to operate at 35.4 GHz on high resistivity (3000 ohm-cm) silicon substrate.

TABLE 1: DIMENSIONS OF THE COPLANAR PATCH ANTENNA ON MICROMACHINED SUBSTRATE

Side length a (mm)	4.88
Lateral Dimension of cavity (mm^2) in top-plane	5.5×5.5
Lateral Dimension of cavity (mm^2) in bottom-plane	5.88×5.88
Length of feed line L_f (mm)	4.85
Width of feed line W_f (mm)	0.200
Thickness of silicon nitride layer (μm)	3
Thickness of HRS silicon substrate (mm)	0.270

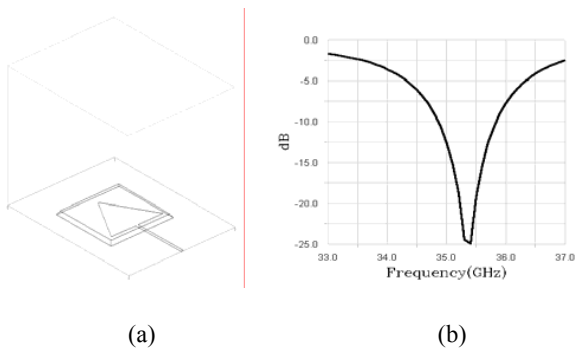



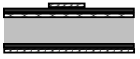





Fig. 2. (a) Multi-layer antenna structure used in simulation and (b) optimised return loss characteristics

The complete sequential process-flow for fabrication of the triangular microstrip patch antenna on a micromachined substrate is shown in Fig.3. The starting wafer is double-side polished $\langle 100 \rangle$ high-resistivity (3000 ohm-cm) silicon wafer of two-inch diameter. The wafer thickness is 270 microns. Silicon nitride films were deposited in an RF (13.56 MHz) diode-sputtering unit (Alcatel QM-311). The pumping system consists of a standard rotary pump, a diffusion pump, and a liquid nitrogen trap. Three-inch diameter stoichiometric target of silicon nitride was used. Sputtering was done in argon atmosphere in "sputter-up" configuration. Prior to sputter deposition, a 0.5-micron of oxide is thermally grown onto the wafers in order to improve the adhesion of sputtered Si_xN_y onto the silicon substrate. The thickness of the thermal oxide is not very critical as only a thin layer will be sufficient to improve the adhesion. The silicon wafers were then clamped on to the substrate holder. The sputtering was done in argon at a pressure of 5 mtorr and 200 Watts of forward RF power. The target to the substrate distance was kept constant at 45 mm for all the deposition runs. No external substrate heating was used during deposition. The film thickness was measured using stylus profiler (Alpha-Step, Tencor Inc.) Typical thickness of sputtered dielectric layer of silicon nitride is 3 μm .

The patch antenna element and the ground metallization is Chrome-Gold (Cr-Au). Typical thickness of the gold is between 1.5-2.5 μm . The chrome-gold metal layers were deposited using RF sputtering. Sputtering was done in argon at a pressure of 5 mtorr and 100 Watts of forward RF power. Front-to-back side alignment procedure was adapted for registration of mutually aligned patterns on the two sides of the wafer. First, front-side Au-metallization was patterned to realize the patch antenna and the feed line, leaving underneath chrome intact. The reason to adopt this procedure is due to the over-etching of Si_xN_y in Potassium Hydroxide (KOH) solution. Chrome layer acts as an etch-mask to underlying sputtered Si_xN_y layer during anisotropic etching of silicon wafers in KOH solution. In absence of chrome layer, the silicon nitride layer from front-side will get exposed to KOH for at least 4-5 hours. This would etch the silicon nitride and would result in considerable membrane thickness variation. Backside window was opened in SiO_2 -Cr-Au layers to etch away the bulk silicon for the formation of air-cavity beneath the patch. KOH solution (potassium hydroxide: 400 gms, DI water: 600 ml; etching temperature: 80 $^\circ\text{C}$) was used for bulk-micromachining. Isopropyl alcohol (IPA) was added to the KOH solution. KOH etching was carried out in a constant temperature bath with a reflux condenser, required to maintain the concentration and thus the etch-rate of the etchant. On the completion of etching process, air-suspended membranes were obtained. The final step was the removal of front-side chrome layer followed by a final IPA rinse. The fabricated antenna is shown in Fig. 4. Here, the membrane was illuminated from the backside using 60-Watts incandescent bulb.

- (i)  Starting material is oxidized single crystal silicon substrate
- (ii)  Sputter deposit silicon nitride film (membrane material)
- (iii)  Sputter deposit Cr-Au layers (antenna metallization)
- (iv)  Pattern front-side Au metallization (to realize microstrip triangular antenna)
- (v)  Pattern back-side Cr-Au (to open window for bulk-silicon etching)
- (vi)  Bulk-micromachining of silicon substrate
- (vii)  Pattern front-side Cr using top Au layer as etch-mask

 Silicon
  Sputtered Si₃N₄
  Chrome
  Gold

Fig. 3: Process-flow adopted for realizing triangular microstrip patch antenna on suspended Si₃N₄ membrane

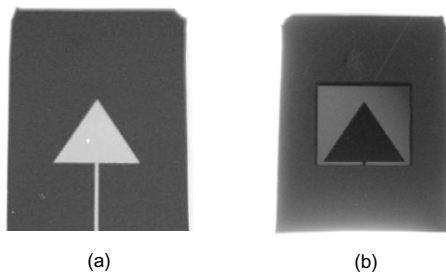


Fig. 4: Photograph of the triangular microstrip antenna on micromachined substrate (a) Top view showing the conductor pattern (b) Bottom view showing the cavity

4. MEASUREMENTS AND RESULTS

For testing the fabricated antenna, it was mounted on a test jig as shown in Fig. 5. The antenna structure was excited using a K-connector (Tensolite model no. 230CCSF) to microstrip transition. The centre frequency and bandwidth were obtained

from reflection measurements. The return loss was measured on a Vector Network Analyser (VNA) (Rhodes and Schwarz, Model ZVK-1127.8651.60). The VNA was calibrated from 33-37 GHz using TOSM standards. The measured and simulated return loss characteristics of the triangular micromachined antenna are plotted in Fig. 6(a). Figure 6(b) shows the measured VSWR of the same antenna as a function of frequency. As observed, the simulated and measured data agrees well. The obtained operating frequency was 35.4 GHz and the -10 dB return loss bandwidth ~1.2 GHz. The measured impedance bandwidth, for VSWR ≤ 2 is 4.23 %.

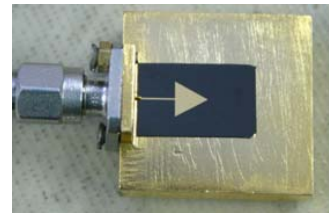
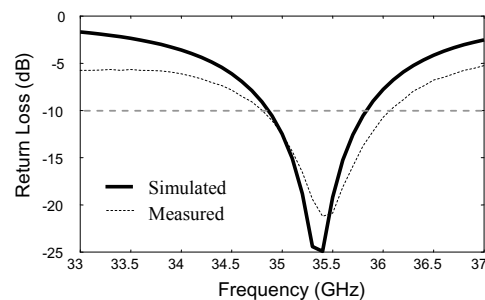
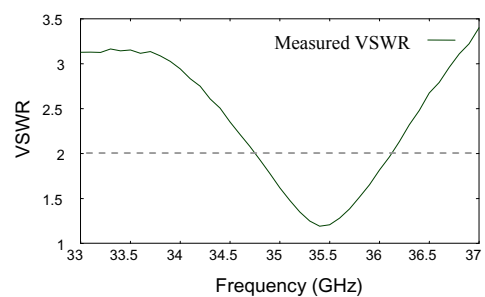


Fig. 5. Photograph of the fabricated triangular microstrip antenna on micromachined substrate mounted on the test jig with K-connector launcher



(a)



(b)

Fig. 6. Characteristics of the fabricated microstrip-fed equilateral triangular patch antenna on micromachined substrate, (a) Measured and simulated return loss, (b) Measured VSWR

5. CONCLUSION

The simulated radiation patterns of the proposed antenna are shown in Fig. 7. From the plots it is evident that the antenna radiates in bore-side direction.

We have presented the design and fabrication of a Ka-band microstrip centrally edge-fed equilateral triangular patch antenna on a suspended 3- μm thick silicon-nitride membrane using silicon bulk-micromachining technique. The complete antenna structure is realized using post-CMOS and post-MMIC compatible metal-dielectric deposition techniques. The measured and simulated results of the antenna show good agreement.

ACKNOWLEDGEMENT

The first author wishes to acknowledge help received in the form of technical discussions held with Dr. Ananjan Basu, Associate Professor. CARE

REFERENCES

- [1] Kai-Fong Lee, Kwai-Man Luk and Jashwant S. Dahele, "Characteristics of the Equilateral Triangular Patch Antenna", *IEEE trans. Antennas and Propagation*, vol. 36, No. 11, pp. 1510-18, Nov 1988.
- [2] Debatosh Guha and Jawad Y. Siddiqui, "Resonant Frequency of Equilateral Triangular Microstrip Antenna with or without Air Gap", *IEEE trans. Antennas and Propagation*, vol. 52, No. 8, pp. 2174-77, August 2004.
- [3] I. Papapolymerou, R. F. Drayton, and L. P. B. Katehi, "Micromachined patch antenna", *IEEE Trans. Antennas Propagat.*, vol. 46, pp. 275-283, Feb. 1998.
- [4] R. Garg, P. Bhartia, I. Bahl, A. Ittipiboon, *Microstrip Antenna Design Handbook*, Artech House, 2001.
- [5] Agilent HFSS Version 5.5

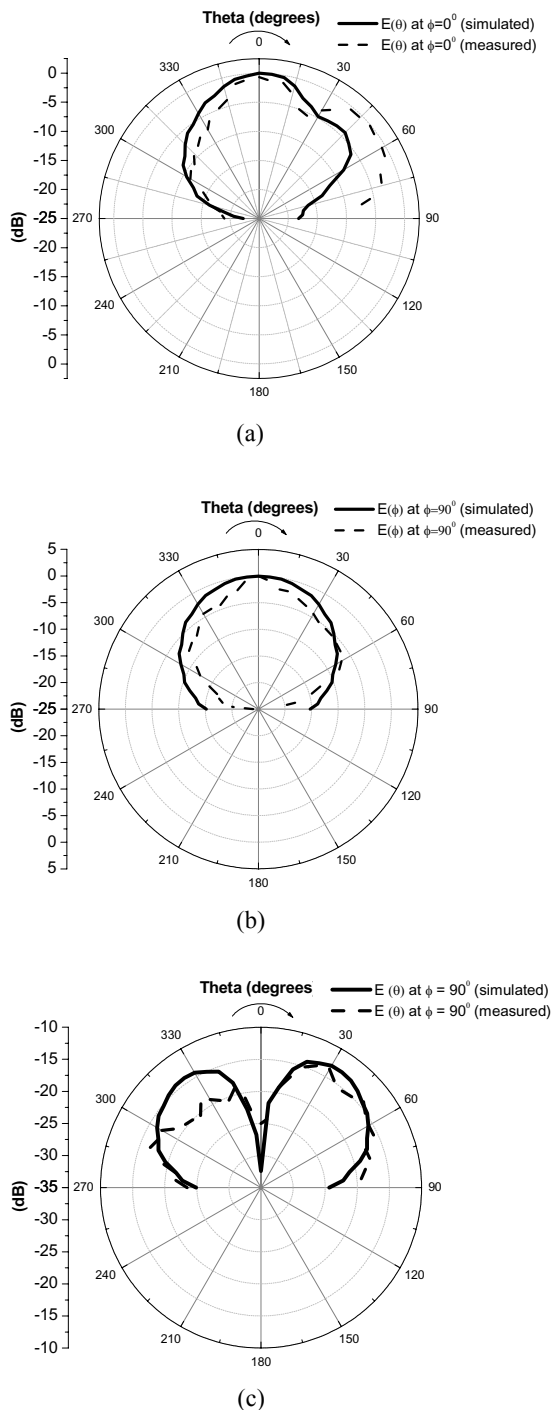


Fig. 7: Radiation pattern of micromachined triangular patch antenna (a) E-plane, (b) H-plane, and, (c) Cross-polarization